ACS Partner Journal

CHEMICAL & BIOMEDICAL IMAGING

Open Access

This article is licensed under CC-BY-NC-ND 4.0

pubs.acs.org/ChemBioImaging

Review

Aptamers as a New Frontier in Molecular Cancer Imaging Technologies

Yingying Li,[#] Tong Shao,[#] Jingyu Kuang, Heqing Yi, Lvyun Zhu,[*] and Xue-Qiang Wang[*]

Cite This: *Chem. Biomed. Imaging* 2025, 3, 267−279

Read Online

ACCESS | Metrics & More | Article Recommendations

ABSTRACT: Molecular imaging has emerged as a transformative tool in cancer diagnosis, enabling the visualization of biological processes at the cellular and molecular levels. Aptamers, single-stranded oligonucleotides with high affinity and specificity for target molecules, have gained significant attention as versatile probes for molecular imaging due to their unique properties, including small size, ease of modification, low immunogenicity, and rapid tissue penetration. This review explores the integration of aptamers with various imaging agents to enhance cancer diagnosis and therapy. Aptamer-based imaging probes offer high sensitivity and real-time visualization of tumor markers. Aptamer-based fluorescence probes and aptamer-conjugated magnetic resonance imaging (MRI) probes, including gadolinium-based contrast agents, improve tumor targeting and imaging resolution. Additionally, aptamers have been utilized in single-photon emission computed tomography (SPECT) and positron emission tomography (PET) imaging to enhance the specificity of radiotracers for cancer detection. Furthermore, aptamer-targeted ultrasound and computed tomography (CT) imaging demonstrate the potential for noninvasive and precise tumor localization. By leveraging the unique advantages of aptamers, these imaging strategies not only improve diagnostic accuracy but also pave the way for image-guided cancer therapies. This review highlights the significant role of aptamers in advancing molecular imaging and their potential to revolutionize cancer diagnosis and treatment.

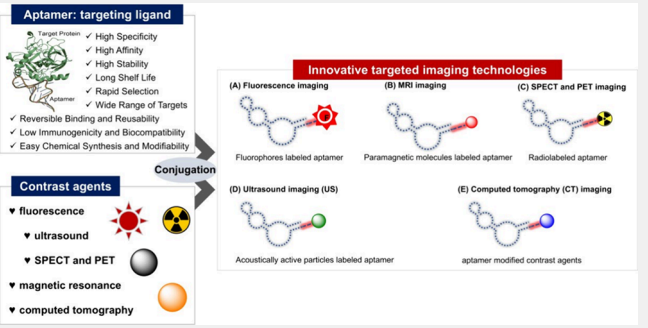

KEYWORDS: *aptamer, Cell-SELEX, specific recognition, precision imaging, targeted therapy, targeted MRI imaging, SPECT imaging, PET imaging, ultrasound imaging, computed tomography imaging*

1. INTRODUCTION

In recent decades, the field of cancer diagnosis has evolved from solely observing morphological changes to visible live imaging techniques. Various imaging technologies, such as optical imaging, magnetic resonance imaging (MRI), ultrasound imaging (US), positron emission tomography (PET), and single-photon emission computed tomography (SPECT), computed tomography (CT) imaging have emerged to monitor and capture subtle changes at the molecular level within biological processes. These technologies aim to unravel complex biological phenomena and provide insights into cancer-related phenomena.[1]

As depicted in Figure 1, aptamers have played a crucial role in molecular cancer imaging by being labeled with different tags or functionalized with biocompatible materials. These modifications have facilitated their widespread application in various imaging modalities. For instance, aptamers labeled with fluorophores enable fluorescence imaging, while those conjugated with paramagnetic molecules enhance MRI imaging. Similarly, the use of ^{99m}Tc-labeled aptamers enables PET imaging, and aptamer-modified gold nanoparticles serve as contrast agents for computed tomography (CT) imaging. These advancements have paved the way for noninvasive molecular imaging of biomarkers, enabling early cancer diagnosis and precise therapeutic interventions.[2]

The discovery and the rapid selection of aptamer greatly accelerate the development of aptamer-based targeted imaging. Thence, this review briefly describes the discovery and development history of aptamers, and then focuses on the recent developments in aptamer-based technologies for targeted cancer imaging. It presents how aptamers, through their versatile labeling and functionalization strategies, offer immense potential for the field of cancer imaging, to enhance our understanding of the disease.

Received: December 17, 2024
Revised: March 30, 2025
Accepted: April 1, 2025
Published: April 9, 2025

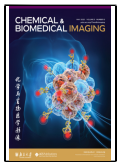

ACS Publications

© 2025 The Authors. Co-published by Nanjing University and American Chemical Society

https://doi.org/10.1021/cbmi.4c00103
Chem. Biomed. Imaging 2025, 3, 267−279

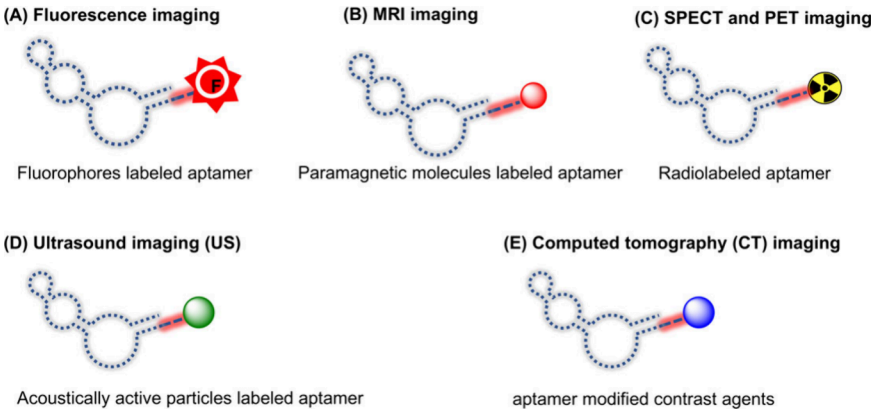

Figure 1. Aptamer-based imaging probes. (A) Fluorophores labeled aptamer for fluorescence imaging. (B) Paramagnetic molecules labeled aptamer for MRI imaging. (C) Radiolabeled aptamer for SPECT imaging and PET imaging. (D) Acoustically active particles labeled aptamer for ultrasound (US) imaging. (E) Aptamer modified contract agents for computed tomography (CT) imaging.

2. APTAMER AND CELL-SELEX TECHNOLOGY

Discovery of Aptamers

The discovery of aptamers could date back to the early 1980s, when researchers studied human immunodeficiency virus type 1 (HIV-1) and adenovirus. They found that the activation of HIV-1 gene expression relies on the interaction between the viral Tat protein and a specific RNA sequence known as TAR (Trans-activation Response element), which is situated at the 5′ end of all viral mRNAs.[3] Subsequently in 1990, the groundbreaking work by Eli Gilboa's group demonstrated that TAR aptamer could bind and inhibit the activity of Tat, thus establishing TAR as a potential therapeutic agent (Figure 2).[4]

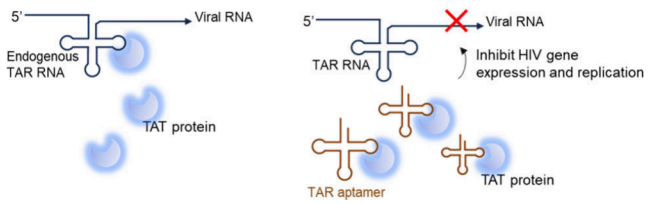

Figure 2. Schematic illustration of the TAR aptamer that serves as a therapeutic agent by preventing the Tat protein from binding the endogenous TAR RNA.

Around the same time, the laboratories of Gold and Szostak independently developed experimental evolution methods for selecting functional nucleic acid molecules that could specifically bind to their target molecules, which was called SELEX (Systematic Evolution of Ligands by Exponential Enrichment). Using SELEX, they identified an RNA sequence from a pool containing 65,536 species. This specific RNA sequence exhibited a high affinity for binding to T4 DNA polymerase, thereby inhibiting its replicative function.[5] The lab led by Szostak coined the term "aptamer" (derived from the Latin word "*aptus*", meaning fit, and the Greek word "*meros*", meaning region) for these functional nucleic acid–based sequences. They developed an *in vitro* selection method that enabled the evolution and isolation of RNA sequences capable of binding to various organic dyes from an initial pool containing 10^{10} random RNA sequences.[6] Since these pioneering discoveries, aptamer research has rapidly advanced.[7]

SELEX Technology

Over time, several SELEX-centered strategies have been devised to generate aptamers that specifically bind to a wide range of targets, including metal ions, small molecules, peptides, proteins, living cells, and tissues.[8] While conventional SELEX methods, such as Capillary Electrophoresis-SELEX and Magnetic Bead-Based SELEX, rely on knowledge of the target molecules, they may encounter difficulties when the purified protein does not adopt a stable conformation or when the native protein exists as a complex.[9] In light of these challenges, the whole cell-based SELEX method, known as Cell-SELEX, has been developed to overcome the limitations of traditional technologies.[10,11]

Cell-SELEX employs living cells as targets, allowing for aptamer screening without prior knowledge of the exact targets present in the utilized cell lines. This approach proves particularly advantageous in biomarker discovery. Furthermore, Cell-SELEX capitalizes on the differences in biomarker expression levels between two populations of cells, thereby reducing the need for tedious experimental procedures associated with target identification and selection.

Cell-SELEX Technology

The Cell-SELEX technology is a highly effective method for selecting aptamers with high affinity and specificity toward target cell lines.[12] The process begins by generating a pool of nucleic acids, which contains up to 10^{16} DNA sequences. This large pool ensures a high diversity, enabling the formation of distinct secondary and tertiary structures that can interact with the membrane proteins of the target cells. As shown in Figure 3, the Cell-SELEX process consists of several key operations, including positive selection, counter selection, and the polymerase chain reaction (PCR) process. First, the target cells are incubated with a library of single-stranded DNA (ssDNA). The unbound sequences are then removed, and the bound sequences are then eluted and collected. These bound sequences are subsequently incubated with a negative control cell line to eliminate any nonspecifically binding sequences. The remaining sequences, which specifically bind to the target cells, are collected and amplified exponentially using PCR. This amplification step generates an evolved DNA pool that can be used for the next round of selection. Due to the occurrence of nonspecific binding events during the selection process, multiple rounds of selection are performed until a stable binding profile is achieved. Flow cytometry is commonly

https://doi.org/10.1021/cbmi.4c00103
Chem. Biomed. Imaging 2025, 3, 267−279

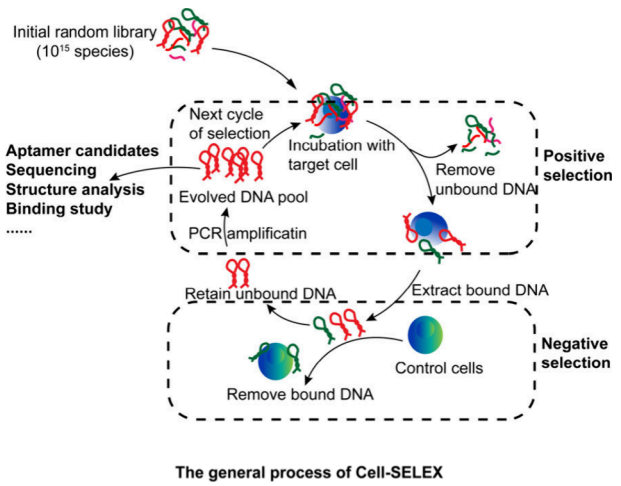

Figure 3. Schematic illustration of the general process of Cell-SELEX for aptamer generation.

employed to assess binding profiles. Once the enriched sequences demonstrate sufficient affinity and specificity toward the target cell lines, the DNA pool is cloned and sequenced to identify candidate aptamers. Additionally, predicting the secondary structure of these candidates provides insights into their interaction with proteins. Based on comprehensive evaluations using flow cytometry or confocal imaging, one aptamer sequence is typically selected for further optimization and application studies.

In recent years, advancements in Cell-SELEX have led to the development of 3D Cell-SELEX, cancer tissue-based SELEX, and *in vivo* SELEX. These variations have facilitated the application of aptamers in more complex biological systems, allowing for their use in a wide range of research areas.[13,14] Many important disease-related cells and cell surface proteins are present at low abundance, posing challenges for aptamer selection. Traditional screening and PCR amplification methods often yield aptamers targeting highly abundant proteins, while those targeting low-abundance proteins are overlooked. To address this issue, the Tan group introduced a digital DNA sequencing strategy known as DiDS selection in 2024.[15] By integrating advanced techniques such as ultra-sensitive DNA barcoding, UMI (Unique Molecular Identifier) labeling, and high-throughput digital DNA sequencing, DiDS selection enables aptamer identification through a single-round, single-cell selection process. This innovative method not only simplifies the selection process but also ensures comprehensive aptamer characterization, paving the way for improved applications in areas such as targeted therapeutics and diagnostics. Using the DiDS selection strategy, the Tan group successfully identified high-quality RNA aptamers

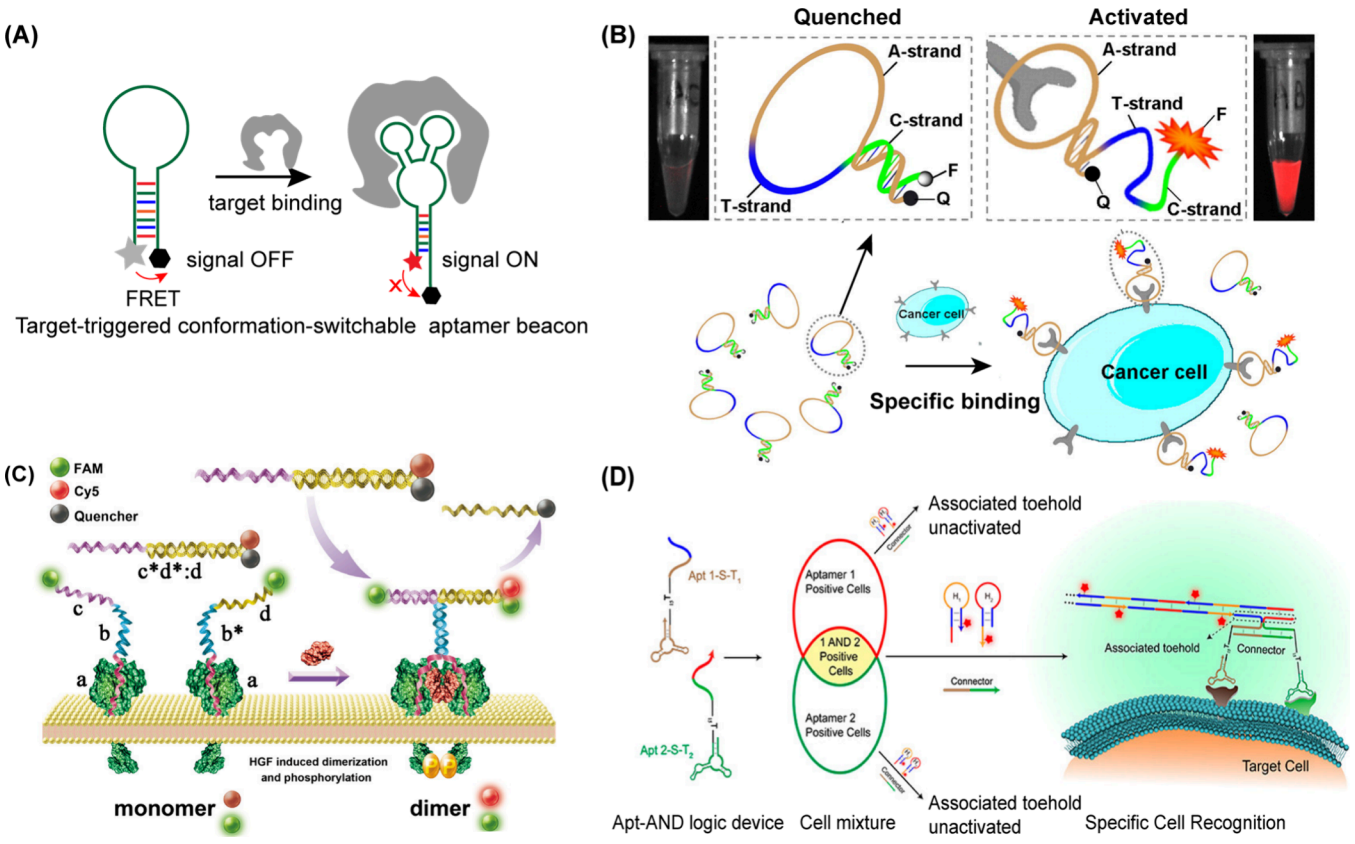

Figure 4. (A) Target-triggered conformation-switchable aptamer beacon. Reproduced with permission from ref 21. Available under a CC-BY-NC license. Copyright 2016 Royal Society of Chemistry. (B) Schematic representation of the novel strategy for in vivo cancer imaging using an activatable aptamer probe (AAP) based on cell membrane protein-triggered conformation alteration. Reproduced with permission from ref 22. Copyright 2011 National Academy of Sciences. (C) Schematic illustration of the principle of imaging protein dimerization on the cell membrane by aptamer recognition and proximity-induced DNA assembly. Reproduced with permission from ref 23. Copyright 2018 American Chemical Society. (D) System design and operational mechanism of dual-aptamer-based AND logic device for cell identification and isolation. Reproduced with permission from ref 25. Copyright 2019 American Chemical Society.

https://doi.org/10.1021/cbmi.4c00103
Chem. Biomed. Imaging 2025, 3, 267−279

targeting the human colon cancer cell line HCT-8 in just two rounds of selection. Furthermore, they demonstrated the method's versatility by isolating six RNA aptamers for the mouse myoblast cell line C2C12 in only one round of selection.[16] This groundbreaking approach facilitates rapid RNA aptamer screening across diverse cell lines, significantly enhancing the potential for RNA aptamer discovery in biomedical research, clinical applications, and precision medicine.

Despite the above success, most aptamers target cell membrane proteins, with few focusing on transcription factor (TF)-DNA interactions. To address this gap, in 2024, Tan group introduced Blocker-SELEX, a structure-guided rational design strategy aimed at developing inhibitory aptamers (iAptamers) that disrupt TF protein−protein interactions.[17] This method involves screening a single-stranded DNA (ssDNA) library against TF complex structures, leading to the identification of aptamers that block specific TF interactions, such as those between SCAF4/SCAF8 and RNAP2 proteins. These iAptamers, when tested in tumor cells, showed the ability to alter cell transcript profiles, disrupt RNA splicing, reduce cell proliferation, and increase apoptosis. The strategy was also successfully applied to develop iAptamers targeting the MYC oncogenic protein. With ongoing improvements in nucleic acid delivery technologies, these aptamers could become crucial tools in both basic research and clinical settings.

3. APTAMER-BASED FLUORESCENCE IMAGING

Aptamer beacons are commonly formulated by directly modifying them with fluorophores that emit signals in different wavelengths or attaching to nanoparticle-based optical probes.[18] In 2005, the Bryan M. Clary group incorporated cyanine dye 5 (Cy5) into an RNA aptamer to specifically image the endogenous integrin $\alpha v\beta 3$.[19] Although Cy5-conjugated aptamers provide stable fluorescence signals, these "always-on" probes suffered from high background noise and limited contrast in live imaging. To address these challenges, the concept of molecular aptamer beacons was developed for more accurate imaging.[20]

The Tan group designed an activatable aptamer probe (AAP) for detecting protein tyrosine kinase 7 (PTK7), an overexpressed membrane protein in living CCRF-CEM cells.[21] The AAP comprised a fluorescent donor (fluorophore FAM) and an acceptor reporter (black hole quencher 1, BHQ1) at its termini. Upon binding to PTK7 on the target cancer cell membrane, the conformation of the AAP switched, activating the fluorescence signal and resulting in significantly higher fluorescence intensity (Figure 4A, 4B).[22] The signal-to-background ratio of the aptamer beacon was approximately 2.5 times higher than that of the always-on probe in CCRF-CEM cells. The AAP also exhibited substantially improved contrast compared to the always-on probe in CCRF-CEM tumor-bearing mice. Compared to the specific tagging of cancer cells, imaging the dynamic movement of proteins on the cell membrane poses greater challenges

To overcome this, aptamer-based nanodevices have been designed to perform logical operations on fluorescence signals based on the DNA strand replacement reaction of aptamers. For example, Tan and colleagues utilized a 40-mer DNA aptamer that binds to the mesenchymal epithelial transition (Met) receptor as a recognition probe to monitor the dimerization of target Met receptor monomers (Figure 4C).[23] The dimerization of receptor proteins brings two aptamer probes close to each other, triggering a dynamic DNA self-assembly process that results in the formation of a DNA duplex. This process leads to the fluorescence recovery of Cy5. This intelligent design enables real-time imaging of the two distinct states (monomer or dimer) of a receptor protein on the living cell membrane, providing a novel strategy for investigating dynamic protein movement and interactions.

Furthermore, significant efforts have been dedicated to developing imaging technologies for detecting intercellular interactions via aptamer beacon. In 2016, Nan Zhang and colleagues reported the selection of the M17A2 aptamer using Cell-SELEX technology.[24] Once this aptamer specifically binds to the intercellular connections associated with cell−cell crosstalk, the fluorescence signal would appear. The M17A2 aptamer differs from previously reported aptamers, highlighting its potential as a new probe for investigating intercellular connections and cell−cell communications.

The specific imaging and isolation of subpopulations of cancer cells from a heterogeneous cell pool are crucial for personalized medicine and biomedical engineering. In 2019, Xu Chang and colleagues developed a multiple-aptamer-based DNA logic device capable of performing cancer cell isolation and accurate imaging in a cell mixture.[25] As pictured in Figure 4D, when the targeting receptors are present in the subpopulation of cells simultaneously, the APT-S-T construct binds to the cell membrane. Through the H1 and H2 hairpin probes, the toehold of the APT-S-T construct is connected to the connector, leading to the generation of fluorescence outputs for the target cell subtypes. This process occurs in a single step and requires fewer fluorescence channels, providing a more efficient and streamlined approach for imaging and isolating specific cell subtypes.

Based on the foundational research in in vitro imaging, a study by Fangzhou et al. demonstrated the use of fluorescence-labeled aptamers in vitro.[26] Specifically, the 56-nt aptamer XQ-2d, which specifically recognizing transferrin receptor 1 (TfR1, also known as CD71), was labeled with fluorophores (FAM or Cy5) and modified with PEG5000-azobenzene-NHS that could response to hypoxia, here acting as a caging moiety of conditional recognition. This modified aptamer was exhibited high specificity and binding affinity in vitro, and its efficacy was further validated in a tumor-bearing mice model, where it successfully facilitated in vivo tumor visualization using fluorescence imaging. This example highlights the critical role of in vitro studies as a preliminary step in the development of aptamer-based imaging agents intended for in vivo applications. Following this advancement, fluorescence-labeled nucleic acid aptamer imaging has been increasingly utilized in vivo, particularly in the realm of aptamer-drug conjugates (ApDCs).[27,28]

4. APTAMER-BASED MAGNETIC RESONANCE IMAGING (MRI)

Since the 1970s and 1980s, magnetic resonance imaging (MRI) has evolved into a widely used medical imaging technique in clinical radiology. It generates detailed images of the body by detecting the interaction of protons (^{1}H) in tissue water or certain atomic nuclei within the body.[29,30] The underlying principle is that different tissues exhibit varying relaxation times when subjected to a powerful magnet and radiofrequency energy.[31] Exogenous contrast agents can be used to further enhance the imaging process by selectively

https://doi.org/10.1021/cbmi.4c00103
Chem. Biomed. Imaging 2025, 3, 267−279

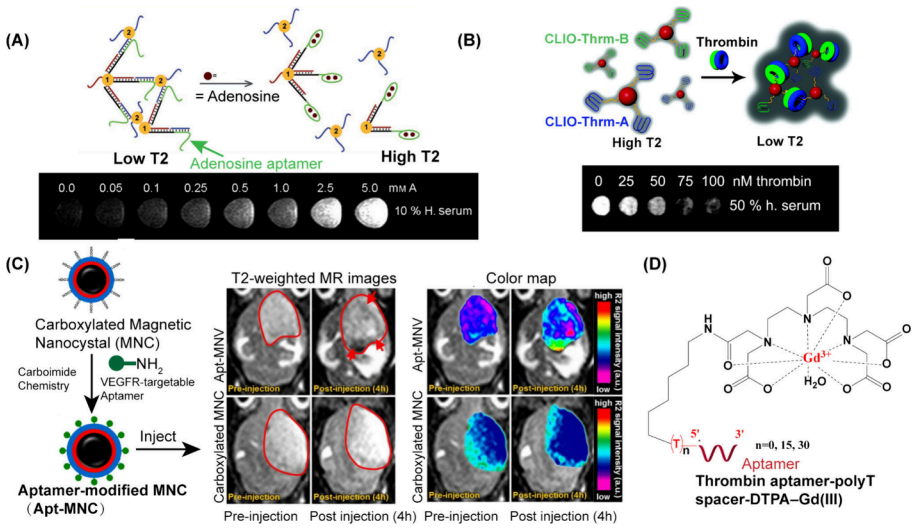

Figure 5. (A) Smart "turn-on" magnetic resonance contrast agents based on aptamer-functionalized SPIONs. Reproduced with permission with permission from ref 36. Copyright 2007 Wiley-VCH Verlag GmbH & Co. KGaA, Weinheim. (B) MRI detection of thrombin with aptamer functionalized superparamagnetic iron oxide nanoparticles. Reproduced with permission with permission from ref 37. Copyright 2008 American Chemical Society. (C) Thrombin aptamer-15 polyT spacer-DTPA-Gd^{3+}. Reproduced with permission from ref 38. Copyright 2013 Kim et al., licensee Springer. (D) *T2*-weighted MR images and their color map for VEGFR2-expressing mouse model with intravenous injection of Apt-MNC or carboxylated MNC (red line: brain tumor; red arrow: contrast enhanced site).

shortening the relaxation time of proton spins, either in the longitudinal direction (T1 relaxation) or in the transverse direction (T2 relaxation), under an external magnetic field. Aptamer-conjugated paramagnetic molecules, such as superparamagnetic iron oxide nanoparticles (SPIONs)[32] and gadolinium-containing compounds,[33−35] are commonly employed as exogenous contrast agents to enhance the MRI signals. The utilization of aptamers in conjunction with contrast agents in MRI provides a valuable tool for enhancing the sensitivity and specificity of imaging, leading to improved diagnostic capabilities.

Aptamer-Conjugated SPIONs as Contrast Agents

The effectiveness of SPION clusters in reducing the T2 relaxation time, leading to a darker T2-weighted MR image, has been reported. The Yigit group developed a method for detecting adenosine using adenosine aptamer-modified SPION clusters through hybridization (Figure 5A). When these clusters encounter increased concentrations of adenosine in human serum (10%), the adenosine aptamer binds to adenosine, causing the cluster to disassemble and resulting in a higher T2 compared to the clusters alone.[36] In another study, aptamer-functionalized SPIONs were utilized to detect thrombin via MRI.[37] The formation of clusters through the interaction of aptamers with thrombin caused a decrease in MR image brightness (Figure 5B). The contrast change in the T2-weighted MR image demonstrated the specificity of the system for thrombin detection, with a concentration sensitivity of 10 nM.

Figure 5C shows the successful application of VEGFR2-targeting aptamer-modified carboxylated SPIONs (referred to as Apt-MNC) in MRI. These particles exhibited a high MR signal (saturation magnetization value of 98.8 emu g^{-1} Fe at 1.5 T) and demonstrated efficient detection of VEGFR2.[38] Numerous other aptamer-SPION conjugates have also been developed for target detection using MRI technology. For instance, aptamer$_{\alpha v\beta 3}$-conjugated SPIONs (Apt$_{\alpha v\beta 3}$-MNPs) were designed for the detection of integrin expressed in cancer cells.[39] SPIONs conjugated to aptamer M17 were used for MMP14-positive cancer imaging.[40] Biotin-labeled aptamer N55 was coupled with commercially available SPIONs (Dynabeads MyOne Streptavidin C1) to detect inflamed endothelial cells.[41] Additionally, double-stranded AP1 aptamer-tagged SPIONs were employed to detect transcription factor proteins AP-1 in live mice using MRI technology.[42] Magnetic carboxymethyl cellulose nanoparticles modified with endoglin aptamer (mEND-Fe_3O_4@CMCS) were developed as an MRI nanoprobe targeting endoglin in hepatocellular carcinoma. These nanoparticles selectively accumulated at the tumor site and displayed enhanced contrast in tumor tissue in mice.[43]

Apart from imaging specific targets using aptamer-modified SPIONs, there have been advancements in engineering targeting probes that enhance MRI efficacy while incorporating model anticancer agents for targeted therapy. SPIONs functionalized with PSMA (prostate-specific membrane antigen) targeting aptamer and loaded with doxorubicin (DOX) were developed as prostate cancer-specific nanotheranostic agents. These nanotheranostics achieved tumor-selective drug delivery effects in an LNCaP xenograft mouse model, demonstrated by T2-weighted MRI both in vitro and in vivo.[44] Similarly, CMC-MNPs conjugated with epithelial cell adhesion molecule (EpCAM) aptamer demonstrated in vitro MR imaging capabilities and codelivery of DOX for cancer cell killing.[45] In a recent study, a self-assembly strategy was used to encapsulate both docetaxel (Dtxl) and SPIONs into a triblock copolymer modified with Wy5a aptamer. Both in vitro and in vivo studies showed that these nanoparticles enhanced antitumor efficacy and improved MRI contrast against castration-resistant prostate cancer.[46]

Aptamer-Based Gadolinium-MRI Contrast Agents

Ga^{3+} is a commonly used agent for MRI contrast imaging, often combined with multidentate ligands such as diethylenetriaminepentaacetic acid (DTPA), 1,4,7,10-tetraazacyclododecane1,4,7,10-tetraacetic acid (DOTA), and others.[33−35]

https://doi.org/10.1021/cbmi.4c00103
Chem. Biomed. Imaging 2025, 3, 267−279

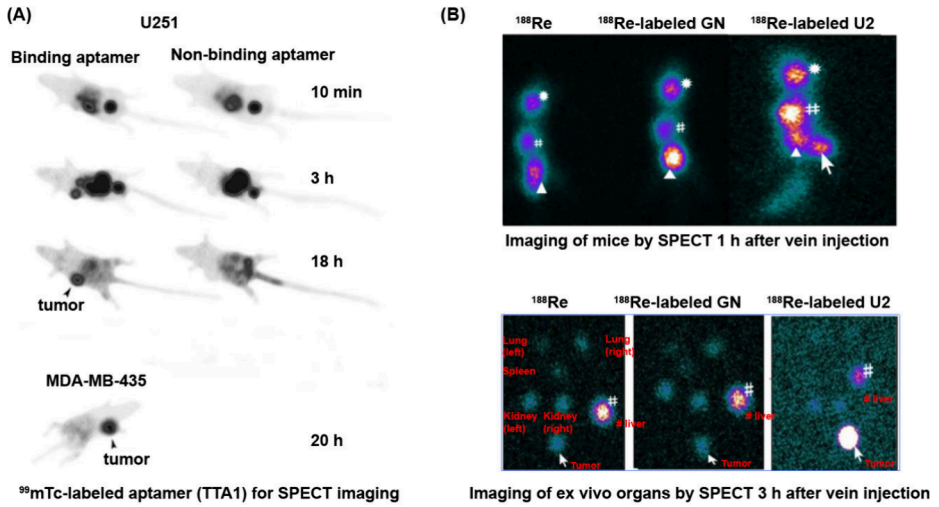

Figure 6. (A) Aptamer-based g-camera images of U251 tumor-bearing mice and breast tumors generated using the cell line of MDA-MB-435. Reproduced with permission from ref 49. Copyright 2006 Society of Nuclear Medicine. (B) Upper: Imaging of mice by SPECT 1 h after tail vein injection of free ^{188}Re (left), ^{188}Relabeled GN (middle) and ^{188}Relabeled U2 (right). Lower: Corresponding imaging of ex vivo organs by SPECT 3 h after tail vein injection of free ^{188}Re (left), ^{188}Relabeled GN (middle) and ^{188}Relabeled U2 (right). Reproduced with permission from ref 50. Copyright 2014 Wu et al.

Conjugation of thrombin targeting aptamer-Ga^{3+} (with DTPA as the ligand for Gd^{3+}) has shown enhancements of 35 ± 4% at 9.4 T and 20 ± 1% at 1.5 T, thanks to the target binding ability of the aptamer (Figure 5D).[47] GBI-10 aptamer-modified liposomes loaded with gadolinium (Gd) have demonstrated noticeable enhancements in T1-weighted MR images compared to commercially available Gd-DTPA.[33] By conjugating aptamers and imaging reporters (Gd^{3+}-DTPA) onto a G5 dendrimer, a nanoprobe was developed for targeting hepatocellular carcinoma (HCC). This nanoprobe enabled the delineation of orthotopic HCC xenografts with diameters as low as 4 mm, facilitating the detection of small HCC lesions for surgical intervention.[34] Another macromolecular MRI contrast agent, AS1411-G2(DTPA-Gd)-SS-PR, was created using α-cyclodextrin (α-CD) polyrotaxane modified with second-generation lysine dendron structures via click chemistry. This agent carried high payloads of Gd chelates and AS1411. In xenograft MCF-7 tumor-bearing mice, AS1411-G2(DTPA-Gd)-SS-PR exhibited significant contrast enhancement in the tumor region compared to the surrounding tissue within 0.5 h after injection. The longitudinal relaxivity of AS1411-G2(DTPA-Gd)-SS-PR was measured to be 11.7 $mM^{-1}s^{-1}$, nearly 2 times higher than that of commercially available Gd-DTPA.[35]

5. APTAMER-BASED SPECT AND PET IMAGING

SPECT (Single Photon Emission Computed Tomography) and PET (Positron Emission Tomography) are nuclear medicine imaging techniques that provide valuable metabolic and functional information. SPECT uses gamma-ray emissions from radioactive tracers that are preinjected into patients, while PET also utilizes radiopharmaceuticals to create images. Currently, there are typically two prominent radionuclides employed in clinical nuclear imaging: (1) SPECT, which employs γ-emitting radionuclides, including ^{99m}Tc ($t_{1/2}$: 6 h, physical half-life), ^{123}I ($t_{1/2}$: 13.2 h), ^{67}Ga($t_{1/2}$: 3.3 d), and ^{111}In ($t_{1/2}$: 2.8 d); (2) PET, which uses β^+-emitting radionuclides, including ^{18}F ($t_{1/2}$: 109.8 min), ^{11}C ($t_{1/2}$: 20.4 min), ^{13}N ($t_{1/2}$: 9.96 min), ^{15}O ($t_{1/2}$: 2.03 min), ^{68}Ga ($t_{1/2}$: 68 min), ^{82}Rb ($t_{1/2}$: 75 s), ^{64}Cu ($t_{1/2}$: 12.7 h), and ^{89}Zr ($t_{1/2}$: 78.1 h). Both techniques offer excellent tissue penetration capabilities compared to other radionuclide-based imaging methods. However, there are certain limitations associated with contrast agents used in clinical SPECT and PET imaging. These include a lack of specificity toward pathological tissue and potential toxicity resulting from their accumulation in certain tissues. To potentially address these drawbacks, researchers have developed aptamer-based targeting agents modified with multidentate ligands for complexing with radioisotopes. These novel agents aimed to improve the accuracy of biomedical imaging.

Radiolabeled Aptamer for SPECT Imaging

The use of aptamers in SPECT imaging was first reported in the late 1990s. In one study, Josephine and colleagues reported the in vivo imaging of inflammation in a rat model using a ^{99m}Tc-labeled aptamer (NX21909) that specifically binds to activated neutrophils.[48] Compared to the clinically used IgG-mediated inflammation imaging technology, the ^{99m}Tc-labeled aptamer demonstrated a significantly improved target-to-background (T/B) ratio (4.3 ± 0.6 at 2 h) compared to IgG (3.1 ± 0.1 at 3 h). The rapid clearance of the aptamer from the peripheral circulation contributed to this improved T/B ratio, demonstrating the feasibility of using aptamers for diagnostic imaging.

In 2006, a ^{99m}Tc-labeled aptamer (TTA1) targeting the fibrinogen-like domain of tenascin-C was used for in vivo delivery of radioisotopes.[49] The ^{99m}Tc-labeled aptamer showed much higher tumor uptake compared to a control aptamer with rapid blood clearance (1.19 vs 0.04%ID/g at 3 h). SPECT imaging with an aptamer-based γ-camera revealed that U251 glioblastoma tumors were faintly visible at 10 min, prominent at 3 h, and showed the strongest signal at 18 h (Figure 6A). In these SPECT imaging studies, ^{99m}Tc exhibited advantages such as a suitable half-life, appropriate gamma photon energy, availability, and low cost.

Apart from ^{99m}Tc, other radionuclides like ^{188}Re and ^{111}In have also been conjugated with aptamers for specific molecular imaging. For example, a ^{188}Relabeled U2 aptamer was tested in

https://doi.org/10.1021/cbmi.4c00103
Chem. Biomed. Imaging 2025, 3, 267−279

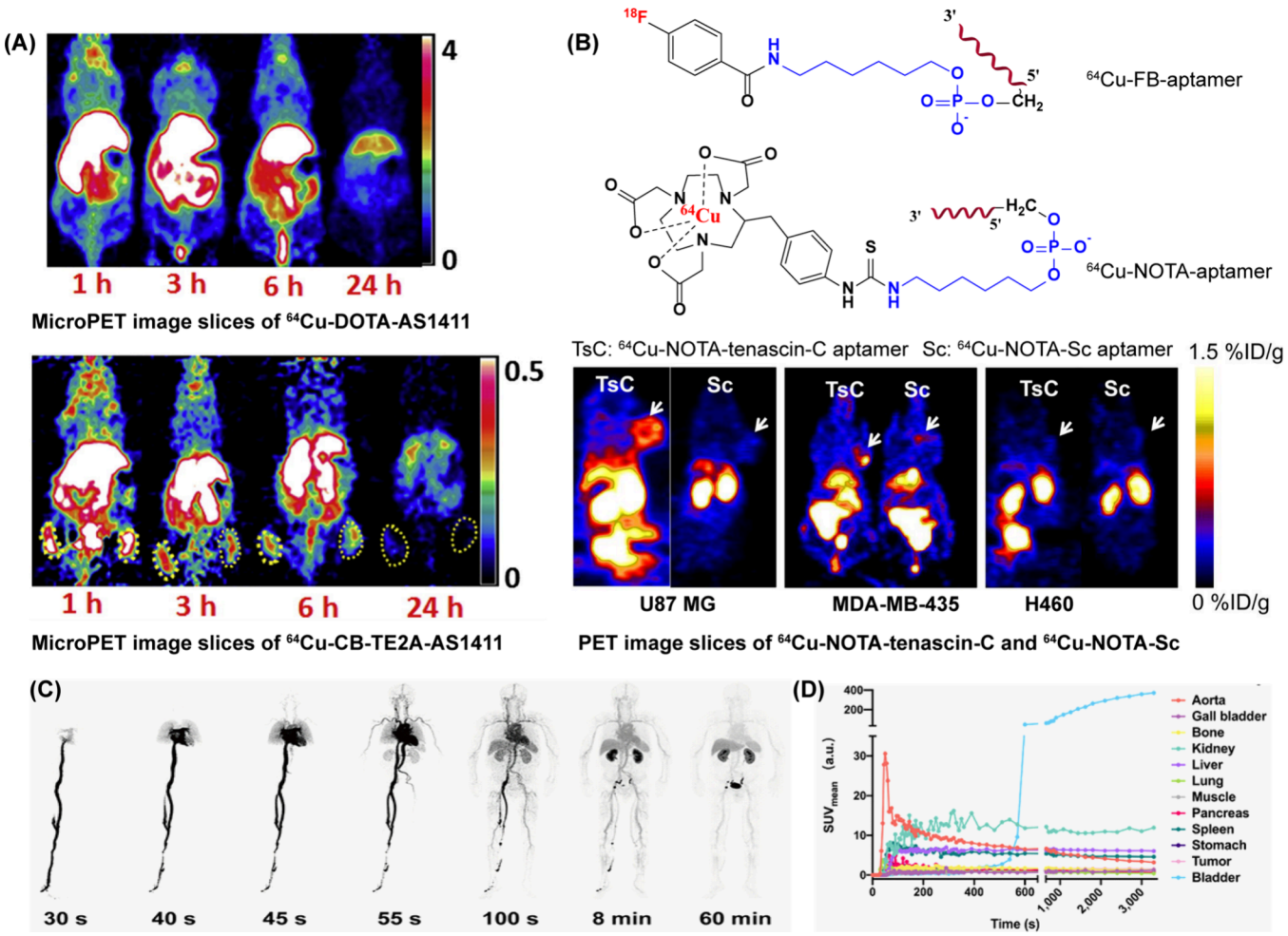

Figure 7. (A) Coronal view of microPET image slices obtained at different time points for ^{64}Cu-DOTA-AS1411 and ^{64}Cu-CB-TE2A-AS1411 (% ID/g). Reproduced with permission from ref 60. Copyright 2014 Elsevier Inc. (B) Representative coronal PET images of ^{64}Cu-NOTA-tenascin-C aptamer and ^{64}Cu-NOTA-Sc aptamer in different tumor models (tenascin-C-positive [U87MG and MDA-MB-435] and tenascin-C-negative [H460]) at 6 h after injection. White arrows represent tumor location. Reproduced with permission from ref 61. Copyright 2015 the Society of Nuclear Medicine and Molecular Imaging, Inc. (C) Whole-body dynamic PET imaging of ^{68}Ga-NOTA-SGC8-injected patient at different time points postadministration, including 30, 40, 45, 55, and 100 s up to 60 min. Reproduced with permission from ref 64. Copyright 2023 Ding Ding et al. (D) Quantitative time-radioactivity curves of major organs according to dynamic PET acquisition. Reproduced with permission from ref 64. Copyright 2023 Ding Ding et al.

a glioblastoma xenograft tumor model with overexpressed epidermal growth factor receptor variant III (EGFRvIII) in mice.[50] The ^{188}Relabeled U2 showed significantly enhanced accumulation in U87-EGFRvIII xenograft tumors compared to free ^{188}Re (Figure 6B). In another study, ^{99m}Tc-MAG-F3B RNA aptamer and ^{111}In-DOTA-F3B RNA aptamer were used to quantitate the biodistribution of human Matrix Metalloprotease-9 (hMMP-9) in A357 tumor-bearing mice.[51] SPECT imaging demonstrated that ^{111}In-DOTA-F3B exhibited significantly higher accumulation at the tumor site compared to the ^{111}In-DOTA-control oligonucleotide.

To improve the pharmacokinetic properties of aptamer-based targeted radiopharmaceuticals, the Sotiris Missailidis group synthesized a novel cyclen-based ligand with a sulfur-containing arm, aiming to enhance the stability of the ligand–metal complex.[52] However, when tetrameric aptamers were used, which improved tumor retention and pharmacokinetic properties compared to monomeric aptamers, there were also side effects observed, including the accumulation of a large amount of radioactivity in the stomach. Hollow gold nanospheres (HAuNS), hollow interior with a thin gold shell (3–6 nm), are second-generation gold nanostructures with small size (outer diameter = 30–50 nm), high number of aptamers/HAuNS (~250).[53] To enhance the pharmacokinetics of aptamers, ^{111}In-labeled aptamers coated HAuNS) were used to target epidermal growth factor receptors (EGFRs) in micro-SPECT/CT imaging of nude mice bearing highly malignant human OSC-19 oral tumors. In comparison to ^{111}In-labeled anti-EGFR antibody conjugated HAuNS or PEG-HAuNS, ^{111}In-labeled apt-HAuNS exhibited significantly higher tumor uptake (3.34 ± 0.44% vs 1.62 ± 0.44%, 0.94 ± 0.44%ID/g).[53]

Radiolabeled Aptamer for PET Imaging

Positron Emission Tomography (PET) is a highly sensitive technology for preclinical and clinical imaging of cancer biology, and it is more sensitive than SPECT.[54] PET is a powerful noninvasive imaging technique that utilizes radiolabeled tracers to visualize metabolic processes within the body. The primary principle behind PET is the detection of γ rays emitted indirectly by a positron-emitting radioisotope

https://doi.org/10.1021/cbmi.4c00103
Chem. Biomed. Imaging 2025, 3, 267–279

administered to the patient. These isotopes decay and emit positrons, which collide with nearby electrons, resulting in the annihilation of both particles and the release of two gamma photons traveling in opposite directions that can be precisely located by the scanner. Essentially, PET "maps" where in the body the tracer is being actively used by cells, providing insight into organ function and disease processes.[55,56]

Although PET's development can be traced back to the mid-1970s,[57,58] the first instance of aptamer-mediated targeted PET imaging was reported in 2011.[59] Researchers evaluated the binding affinity of ^{64}Cu-labeled RNA aptamers (A10−3.2) with different chelators for potential PET imaging. In 2014, the Chin group assessed ^{64}Cu-labeled AS1411 with four chelators DOTA, CB-TE2A, DOTA-Bn, and NOTA-Bn, to explore suitable PET imaging agents both in vitro and in vivo.[60] MicroPET image slices obtained at different time points demonstrated that ^{64}Cu-CB-TE2A-AS1411 may be capable of detecting lung cancer due to its high tumor-to-background ratio, lower liver accumulation, and faster clearance compared to others (Figure 7A). In another study, a tenascin-C targeting aptamer and its nonspecific scrambled aptamer were respectively radiolabeled with ^{18}F and ^{64}Cu to evaluate their in vivo specificity through PET imaging.[61] The authors found that the labeled tenascin-C aptamer exhibited clear visualization in tenascin-C-positive tumors but not in tenascin-C-negative tumors (Figure 7B).

In 2019, a study demonstrated that the ^{18}F-labeled HER2 aptamer exhibited higher accumulation ability in HER2-positive BT474 cell xenografted tumors compared to HER2-negative cell tumors ($p = 0.033$).[62] Both studies proved that targeting aptamers enhance the accumulation ability of aptamer-radiolabeled PET imaging agents. In 2016, the André group evaluated the general biodistribution of ^{68}Ga-labeled HER2 aptamers in mice. However, although a high accumulation of ^{68}Ga-labeled HER2 radioactivity was observed by PET/CT in HER2-positive tumors compared to HER2-negative tumors, ex vivo biodistribution analysis revealed that the high radioactivity in the different blood fractions would affect the quality of PET images by causing high background noise and leading to low image contrast. The research discovered that the major radioactivity present in the blood proteins was due to nonspecific aptamer binding to blood proteins.[63]

In 2023, Tan group, for the first time, conducted a prospective clinical trial through the whole-body dynamic PET real-time, dynamic scanning of ^{68}Ga-NOTA-SGC8 in the human body, and established relevant pharmacokinetic models.[64] The trial proved the targeting specificity of ^{68}Ga-NOTA-SGC8 to PTK-7 positive tumors and dynamically investigated the distribution and metabolism of radiolabeled nucleic acid aptamers through the kidneys via urine (Figure 7C, 7D). This study not only inspired the future development of more nucleic acid aptamer-based PET imaging probes, but also laid a solid foundation for nucleic acid aptamers and the clinical translation of nucleic acid-related medicine.

6. APTAMER-BASED TARGETED ULTRASOUND IMAGING

Ultrasound imaging (US) uses high-frequency sound waves (typically between 1 and 20 MHz) to generate images of the body's interior for investigating pathological processes, including tumors and inflammation. Acoustically active particles, such as nanobubbles, are commonly used as contrast agents for ultrasound. Nanobubbles are nanoscopic gaseous cavities, typically filled with air, that exist in aqueous solutions and have the unique ability to alter the normal properties of water.[65,66] Microbubbles function as ultrasound (US) contrast agents by interacting with ultrasound waves in a way that enhances imaging quality. When an ultrasound wave is applied, bubbles respond by generating signals at harmonic frequencies—these are multiples of the frequency of the stimulating pulse. This interaction occurs because the microbubbles oscillate in response to the pressure changes from the ultrasound wave, leading to the production of distinct harmonic signals.[67]

To perform targeted ultrasound imaging, researchers have developed aptamer-modified nanobubbles as contrast agents. In 2011, the Chih-Kuang group reported that sgc8c covalently modified nanobubbles exhibited enhanced uptake into CCRF-CEM cells, as indicated by cellular US imaging.[68] The same group, one year later, constructed sgc8c aptamer-conjugated and DOX-loaded acoustic droplets (lipid nanobubbles). Cellular US imaging demonstrated that acoustic nanodroplets could selectively recognize CCRF-CEM cells, leading to enhanced cancer cell-killing ability (Figure 8A).[69]

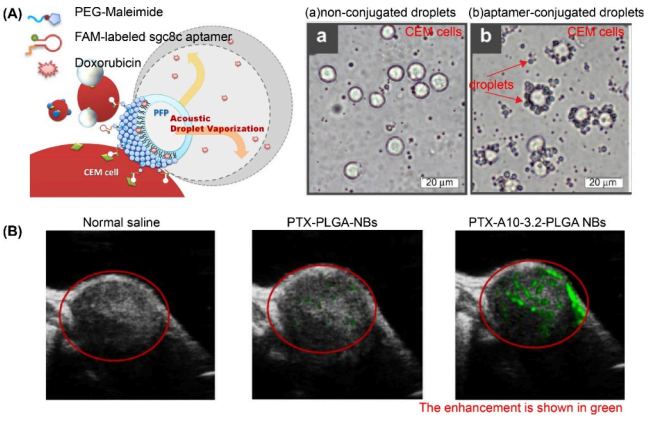

Figure 8. (A) Aptamer-conjugated and DOX-loaded droplets for highly specific targeted therapy (left). Bright-field images showing the targeting capabilities of nonconjugated (a) and aptamer-conjugated droplets (b) in CEM cells (right). Reproduced with permission from ref 69. Copyright 2011 Elsevier Ltd. (B) High-frequency resolution US imaging under contrast mode for PTX−PLGA NBs and PTX-A10-3.2-PLGA NBs in xenograft tumors. The enhancement is shown in green in various groups: the normal saline group, PTX−PLGA NBs group, and the PTX-A10-3.2-PLGA NBs group. Reproduced with permission from ref 72. Copyright 2017 Wu et al, Dove Medical Press Limited.

Matthew A. Nakatsuka and his colleagues developed three thrombin-responsive contrast agents by coupling DNA oligonucleotides to the stabilizing lipid monolayer. In vitro experiments showed that this thrombin-activated microbubble produced ultrasound harmonic signals only when exposed to elevated levels of thrombin.[70] In 2013, in vivo experiments demonstrated that thrombin aptamer cross-linked microbubbles exhibited a 5-fold increase in acoustic activity in an acute thrombosis model in rabbits, whereas the scrambled aptamer cross-linked nanobubbles showed no increase in the acoustic signal.[71] In 2015, the same group improved "smart" nanobubbles by introducing an aptamer, which could differentiate between active and inactive clots for the diagnosis of Deep Venous Thrombosis. The test in a rabbit model

https://doi.org/10.1021/cbmi.4c00103
Chem. Biomed. Imaging 2025, 3, 267−279

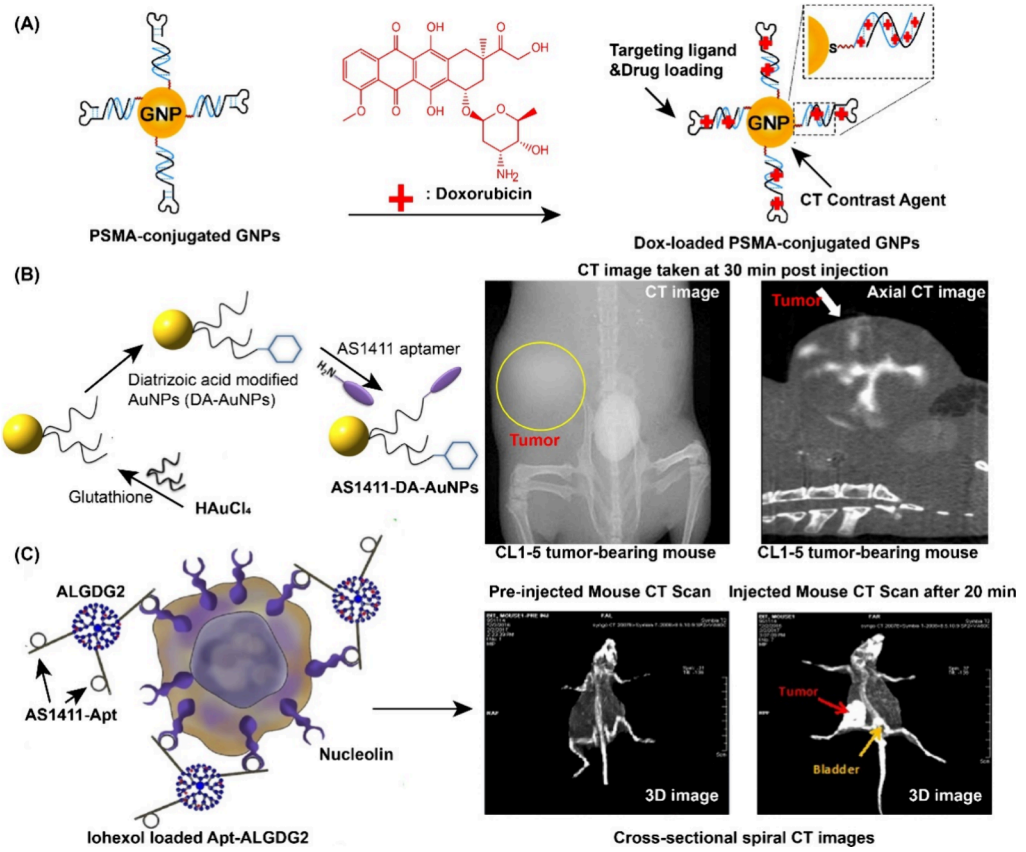

Figure 9. (A) Schematic illustration of the method for preparing DOX-loaded aptamer-conjugated GNPs. Reproduced with permission from ref 75. Copyright 2010 American Chemical Society. (B) (left) The sequential synthetic steps of AS1411-DA-AuNPs. (right) The CT image of the CL1−5 tumor-bearing mouse was taken at 30 min postinjection of AS1411-DA-AuNPs. The location of the CL1−5 tumor was marked by the yellow circle and the axial CT image of the CL1−5 tumor. The location of the CL1−5 tumor was marked by the white arrow. Reproduced with permission from ref 76. Copyright 2015 Cheng-hung Li et al. (C) Cross-sectional spiral CT images of preinjected and injected mice with Apt-ALGDG2-Iohexol after 20 min. The red arrows point to the tumor site in each picture. The yellow arrow shows the bladder site. Reproduced with permission from ref 77. Copyright 2017 Pardis Mohammadzadeh et al.

demonstrated the versatility of "smart" nanobubbles in sensing not only the clotting enzyme thrombin but also other soluble biomarkers in the bloodstream.[67]

The in vivo imaging of aptamer-modified nanobubbles was reported in 2017 by the Zhibiao Wang group.[72] The authors used A10−3.2 aptamer-modified poly(lactide-*co*-glycolic acid) (PLGA) nanobubbles (NBs) that encapsulated paclitaxel (PTX-A10−3.2-PLGA NBs) to target PSMA. High-frequency resolution US imaging of prostate tumor-bearing nude mice preinjected with PTX-A10−3.2-PLGA NBs showed a more concentrated and richer distribution of contrast agent echo signals in the tumor compared to the control PTX−PLGA NBs without targeting ability (Figure 8B).

7. APTAMER-BASED TARGETED CT IMAGING

Computed tomography (CT) imaging is a commonly used medical imaging technique that provides detailed images of the body for diagnostic purposes. It works by capturing the differential absorption of X-rays by various tissues around a single axis of rotation. To enhance the contrast of different soft tissues during a CT scan, water-soluble iodinated contrast agents (such as OmnipaqueTM or Exypaque) are typically used. However, these agents have limitations including nonspecific distribution, rapid clearance, and renal toxicity.[73] Gold nanoparticles (GNPs) have emerged as promising candidates for CT imaging contrast agents due to their stronger X-ray attenuation per atom compared to iodine, a high number of atoms per GNP, and ease of modification with targeting ligands.[74] Consequently, aptamer-functionalized multifunctional GNPs have been designed for targeted CT imaging. For instance, GNPs functionalized with PSMA RNA aptamers have been used for specific imaging of prostate cancer cells, resulting in more than a 4-fold increase in CT intensity in the targeted LNCaP cell line compared to a control PC3 cell line (Figure 9A).[75]

In 2015, a dual-function CT/fluorescent imaging platform was established using nucleolin-targeted AS1411 aptamers and diatrizoic acid-modified fluorescent GNPs. This platform served as a targeted molecular contrast agent for tumor imaging, allowing the simultaneous acquisition of CT and fluorescence images for the colocalization and resection of tumors in CL1−5 tumor-bearing mice (Figure 9B).[76] Additionally, nucleolin-targeting AS1411 aptamer-modified GNPs (Apt-ALGDG2-Iohexol) made the tumor site visible in vivo imaging obtained through cross-sectional spiral CT scanning, as shown in Figure 9C.[77] Numerous other gold-based platforms have been developed for targeted CT scanning, such as Muc-1 aptamer-modified curcumin-loaded PEGylated Au dendrimers (Apt-PEG-AuPAMAM-CUR) for CT imaging of colorectal cancer adenocarcinoma.[78] Another example includes Au-TiO_2 nanoparticles with mitochondria-targeted

https://doi.org/10.1021/cbmi.4c00103
Chem. Biomed. Imaging 2025, 3, 267−279

triphenylphosphine (TPP) and AS1411 aptamers (Au-TiO_2-AS1411-TPP) for organelle-targeted CT imaging.[79]

8. DISCUSSION AND PERSPECTIVE

In the review, we discussed the typical applications of aptamers in targeted imaging. However, there are still drawbacks that limit the *in vivo* application of aptamers, such as rapid clearance from the bloodstream and short circulation times. In comparison to antibodies, which are formed by 20 amino acids, canonical aptamers are composed of two base pair genetic alphabets (A-T and G-C), resulting in reduced diversity. The introduction of artificial bases, which expands the genetic code and enhance the variety and diversity of aptamers.[80−84] Researchers like Anna Marie Pyle et al. have explored modified aptamers containing deoxyuridine (2Nap-dU) substituted at the 5-position with 2-naphthylmethyl, aiming to enhance stability and half-life. Continued efforts to expand the chemical diversity and optimize the stability of aptamers will be crucial for advancing their clinical potential. Certain aptamers with unusual polar and hydrophobic elements have demonstrated high affinity (K_d = 7.3 nM) against IL-1α, showing great potential for clinical applications.[85] As further artificial base pairs are developed, there is hope that aptamers with clinical potential can be selected and expanded, broadening their applications in the clinical setting.This highlights the utility of chemical modifications in SELEX and the development of aptamers. Additionally, it is also important to consider that heavy chemical modification of aptamers can impact their binding affinity. These deficiencies need to be addressed to achieve further clinical applications.

Up until now, significant progress has been made in the development of the technology platform for targeted imaging. There are still many challenges and future prospects that need to be addressed for their clinical application. These challenges include:

(1) Enhanced Target Specificity. Aptamers are susceptible to degradation by serum nucleases, which can lead to off-target effects. Further research is needed to elucidate the precise pharmacological mechanisms of aptamer, including their biodistribution, cellular uptake, and intracellular fate. Understanding these details will optimize their design and selection. Ongoing developments in aptamer selection technologies, such as advanced SELEX methods, could lead to the discovery of highly specific and structurally stable aptamers against novel biomarkers associated with various cancer types. This could facilitate more precise imaging and improve the detection of cancer at earlier stages.

(2) Multiplex Imaging. The ability to label multiple aptamers with different imaging agents could enable simultaneous visualization of multiple biomarkers within a single sample. This multiplex approach would provide comprehensive insights into tumor heterogeneity and the microenvironment, allowing for better understanding and treatment of complex cancers.

(3) Integration with Therapeutic Agents. Future advancements may focus on developing dual-function aptamers that not only serve as imaging agents but also deliver therapeutic payloads (e.g., drugs, RNA therapeutics) directly to target cells. This could create a synergistic effect where imaging and therapy occur concurrently, improving treatment efficacy while allowing real-time monitoring of therapeutic responses.

(4) Nanotechnology Integration. Combining aptamers with nanomaterials could enhance imaging capabilities. For instance, integrating aptamers with nanoparticles that possess unique optical or magnetic properties could improve signal strength and resolution in imaging modalities such as fluorescence, MRI, and CT.

(5) Personalized Medicine Applications. As precision medicine continues to evolve, aptamer-based imaging agents could be tailored to individual patients based on their specific tumor profiles. Incorporating AI and machine learning algorithms into imaging analysis could improve the interpretation of aptamer-mediated images. Advanced computational techniques could help identify subtle patterns in imaging data, aiding in early diagnosis and treatment planning. These personalized approaches could maximize diagnostic accuracy and improve treatment outcomes by ensuring that therapies are directed toward the most relevant targets.

In conclusion, while aptamers hold immense promise for targeted imaging and clinical applications, several challenges must be addressed to fully realize their potential. Overcoming limitations such as rapid clearance, reduced diversity, and susceptibility to degradation will require continued innovation in chemical modifications, SELEX technologies, and the integration of artificial bases. Additionally, advancements in multiplex imaging, therapeutic integration, nanotechnology, and personalized medicine will be pivotal in expanding the clinical utility of aptamers. By addressing these challenges and leveraging emerging technologies, aptamer-based imaging agents can be optimized to provide more precise, effective, and tailored solutions for disease diagnosis and treatment. The future of aptamer applications in targeted imaging is bright, but collaborative efforts across disciplines will be essential to translate these advancements into real-world clinical benefits.

AUTHOR INFORMATION

Corresponding Authors

Lvyun Zhu − *Department of Biology and Chemistry, College of Science, National University of Defense Technology, Changsha 410073, China;* orcid.org/0000-0003-2288-5981; Email: zhulvyun@nudt.edu.cn

Xue-Qiang Wang − *Zhejiang Cancer Hospital, Hangzhou Institute of Medicine (HIM), Chinese Academy of Sciences, Hangzhou, Zhejiang 310022, China; Molecular Science and Biomedicine Laboratory (MBL), State Key Laboratory of Chemo/Bio-Sensing and Chemometrics, College of Chemistry and Chemical Engineering, Aptamer Engineering Center of Hunan Province, Hunan University, Changsha 410082, China;* orcid.org/0000-0003-1631-9158; Email: wangxq@hnu.edu.cn

Authors

Yingying Li − *Department of Biology and Chemistry, College of Science, National University of Defense Technology, Changsha 410073, China*

Tong Shao − *Department of Biology and Chemistry, College of Science, National University of Defense Technology, Changsha 410073, China*

Jingyu Kuang − *Department of Biology and Chemistry, College of Science, National University of Defense Technology, Changsha 410073, China*

Heqing Yi − *Zhejiang Cancer Hospital, Hangzhou Institute of Medicine (HIM), Chinese Academy of Sciences, Hangzhou, Zhejiang 310022, China*

Complete contact information is available at:

https://doi.org/10.1021/cbmi.4c00103
Chem. Biomed. Imaging 2025, 3, 267−279

https://pubs.acs.org/10.1021/cbmi.4c00103

Author Contributions

#Y.L. and T.S. contributed equally.

Notes

The authors declare no competing financial interest.

■ ACKNOWLEDGMENTS

This work was support by the National Natural Science Foundation of China (32171429) and the Natural Science Foundation of Hunan Province (2022JJ30672, 2024JJ9218).

■ ABBREVIATIONS

ApDCs, aptamer-drug conjugates; ADCs, antibody-drug conjugates; SELEX, Systematic Evolution of Ligands by Exponential Enrichment; SPIONs, superparamagnetic iron oxide nanoparticles; MRI, magnetic resonance imaging; US, ultrasound imaging; PET, positron emission tomography; SPECT, single-photon emission computed tomography; MMAE, monomethyl auristatin E; MMAF, monomethyl auristatin F; PTK7, protein tyrosine kinase 7; AAP, an activatable aptamer probe; DTPA, diethylenetriaminepenta-acetic acid; DOTA, 1,4,7,10-tetraazacyclododecane1,4,7,10-tetraacetic acid

■ REFERENCES

(1) Massoud, T. F.; Gambhir, S. S. Molecular imaging in living subjects: seeing fundamental biological processes in a new light. *Genes & development* **2003**, *17* (5), 545−580.
(2) Dougherty, C.; Cai, W.; Hong, H. Applications of aptamers in targeted imaging: state of the art. *Curr. Top. Med. Chem.* **2015**, *15* (12), 1138−1152.
(3) Braddock, M.; Powell, R.; Blanchard, A.; Kingsman, A.; Kingsman, S. HIV-1 TAR RNA-binding proteins control TAT activation of translation in Xenopus oocytes. *FASEB J.* **1993**, *7* (1), 214−222.
(4) Sullenger, B. A.; Gallardo, H. F.; Ungers, G. E.; Gilboa, E. Overexpression of TAR sequences renders cells resisitant to human immunodeficiency virus replicaion. *Cell* **1990**, *63* (5), 601−608.
(5) Tuerk, C.; Gold, L. Systematic evolution of ligands by exponential enrichment: RNA ligands to bacteriophage T4 DNA polymerase. *Science* **1990**, *249* (4968), 505−510.
(6) Ellington, A. D.; Szostak, J. W. In vitro selection of RNA molecules that bind specific ligands. *Nature* **1990**, *346* (6287), 818−822.
(7) Stoltenburg, R.; Reinemann, C.; Strehlitz, B. SELEX-A (r)evolutionary method to generate high-affinity nucleic acid ligands. *Biomol. Eng.* **2007**, *24* (4), 381−403.
(8) Kohlberger, M.; Gadermaier, G. SELEX: Critical factors and optimization strategies for successful aptamer selection. *Biotechnol. Appl. Biochem.* **2022**, *69* (5), 1771−1792.
(9) Darmostuk, M.; Rimpelova, S.; Gbelcova, H.; Ruml, T. Current approaches in SELEX: An update to aptamer selection technology. *Biotechnol. Adv.* **2015**, *33* (6), 1141−1161.
(10) Fang, X.; Tan, W. Aptamers Generated from Cell-SELEX for Molecular Medicine: A Chemical Biology Approach. *Acc. Chem. Res.* **2010**, *43* (1), 48−57.
(11) Sefah, K.; Shangguan, D.; Xiong, X.; O'Donoghue, M. B.; Tan, W. Development of DNA aptamers using Cell-SELEX. *Nat. Protoc.* **2010**, *5* (6), 1169−1185.
(12) Ohuchi, S. Cell-SELEX technology. *Biores. Open Access* **2012**, *1* (6), 265−272.
(13) Mi, J.; Liu, Y.; Rabbani, Z. N.; Yang, Z.; Urban, J. H.; Sullenger, B. A.; Clary, B. M. In vivo selection of tumor-targeting RNA motifs. *Nat. Chem. Biol.* **2010**, *6* (1), 22−24.
(14) Cheng, C.; Chen, Y. H.; Lennox, K. A.; Behlke, M. A.; Davidson, B. L. In vivo SELEX for Identification of Brain-penetrating Aptamers. *Molecular Therapy-Nucleic Acids* **2013**, *2*, No. e67.
(15) Wu, X.; Liu, Y.; Zhang, D.; Yu, J.; Zhang, M.; Feng, S.; Zhang, L.; Fu, T.; Tan, Y.; Bing, T.; Tan, W. Efficient Strategy to Discover DNA Aptamers Against Low Abundance Cell Surface Proteins in Scarce Samples. *J. Am. Chem. Soc.* **2024**, *146* (39), 26667−26675.
(16) Zhang, D.; Liu, Y.; Huang, H.; Fu, T.; Bing, T.; Wu, X.; Tan, W. Streamlining RNA Aptamer Selection via Unique Molecular Identifiers and High-Throughput Sequencing. *Anal. Chem.* **2024**, *96* (42), 16686−16694.
(17) Li, T.; Liu, X.; Qian, H.; Zhang, S.; Hou, Y.; Zhang, Y.; Luo, G.; Zhu, X.; Tao, Y.; Fan, M.; et al. Blocker-SELEX: a structure-guided strategy for developing inhibitory aptamers disrupting undruggable transcription factor interactions. *Nat. Commun.* **2024**, *15* (1), 6751.
(18) Yoon, S.; Rossi, J. J. Targeted molecular imaging using aptamers in cancer. *Pharmaceuticals* **2018**, *11* (3), 71.
(19) Mi, J.; Zhang, X.; Giangrande, P. H.; McNamara, J. O., II; Nimjee, S. M.; Sarraf-Yazdi, S.; Sullenger, B. A.; Clary, B. M. Targeted inhibition of $\alpha v\beta 3$ integrin with an RNA aptamer impairs endothelial cell growth and survival. *Biochem. Biophys. Res. Commun.* **2005**, *338* (2), 956−963.
(20) Tan, W.; Wang, K.; Drake, T. J. Molecular beacons. *Curr. Opin. Chem. Biol.* **2004**, *8* (5), 547−553.
(21) Sun, H.; Tan, W.; Zu, Y. Aptamers: versatile molecular recognition probes for cancer detection. *Analyst* **2016**, *141* (2), 403−415.
(22) Shi, H.; He, X.; Wang, K.; Wu, X.; Ye, X.; Guo, Q.; Tan, W.; Qing, Z.; Yang, X.; Zhou, B. Activatable aptamer probe for contrast-enhanced in vivo cancer imaging based on cell membrane protein-triggered conformation alteration. *Proc. Natl. Acad. Sci. U. S. A.* **2011**, *108* (10), 3900−3905.
(23) Liang, H.; Chen, S.; Li, P.; Wang, L.; Li, J.; Li, J.; Yang, H. H.; Tan, W. H. Nongenetic Approach for Imaging Protein Dimerization by Aptamer Recognition and Proximity-Induced DNA Assembly. *J. Am. Chem. Soc.* **2018**, *140* (12), 4186−4190.
(24) Zhang, N.; Bing, T.; Shen, L.; Song, R.; Wang, L.; Liu, X.; Liu, M.; Li, J.; Tan, W.; Shangguan, D. Intercellular Connections Related to Cell-Cell Crosstalk Specifically Recognized by an Aptamer. *Angew. Chem., Int. Ed.* **2016**, *55* (12), 3914−3918.
(25) Chang, X.; Zhang, C.; Lv, C.; Sun, Y.; Zhang, M.; Zhao, Y.; Yang, L.; Han, D.; Tan, W. Construction of a Multiple-Aptamer-Based DNA Logic Device on Live Cell Membranes via Associative Toehold Activation for Accurate Cancer Cell Identification. *J. Am. Chem. Soc.* **2019**, *141* (32), 12738−12743.
(26) Zhou, F.; Fu, T.; Huang, Q.; Kuai, H.; Mo, L.; Liu, H.; Wang, Q.; Peng, Y.; Han, D.; Zhao, Z.; Fang, X.; Tan, W. Hypoxia-Activated PEGylated Conditional Aptamer/Antibody for Cancer Imaging with Improved Specificity. *J. Am. Chem. Soc.* **2019**, *141* (46), 18421−18427.
(27) Li, F.; Lu, J.; Liu, J.; Liang, C.; Wang, M.; Wang, L.; Li, D.; Yao, H.; Zhang, Q.; Wen, J.; Zhang, Z.-K.; Li, J.; Lv, Q.; He, X.; Guo, B.; Guan, D.; Yu, Y.; Dang, L.; Wu, X.; Li, Y.; Chen, G.; Jiang, F.; Sun, S.; Zhang, B. T.; Lu, A.; Zhang, G. A water-soluble nucleolin aptamer-paclitaxel conjugate for tumor-specific targeting in ovarian cancer. *Nat. Commun.* **2017**, *8* (1), 1390.
(28) Li, Y.; Peng, Y.; Tan, Y.; Xuan, W.; Fu, T.; Wang, X.-Q.; Tan, W. A new paradigm for artesunate anticancer function: considerably enhancing the cytotoxicity via conjugating artesunate with aptamer. *Signal Transduction Targeted Ther.* **2021**, *6* (1), 327.
(29) Buppenorphine M, N. V. What is an MRI scan and what can it do? *Drug and Therapeutics Bulletin* **2011**, *49* (12), 141−144.
(30) Herzog, H.; Lerche, C. Advances in Clinical PET/MRI Instrumentation. *PET Clinics* **2016**, *11* (2), 95−103.
(31) Rajan, S. S. *MRI: a conceptual overview*. 1998.
(32) Wei, H.; Wiśniowska, A.; Fan, J.; Harvey, P.; Li, Y.; Wu, V.; Hansen, E. C.; Zhang, J.; Kaul, M. G.; Frey, A. M.; Adam, G.; Frenkel, A. I.; Bawendi, M. G.; Jasanoff, A. Single-nanometer iron oxide

nanoparticles as tissue-permeable MRI contrast agents. *Proc. Natl. Acad. Sci. U. S. A.* **2021**, *118* (42), No. e2102340118.
(33) Zhang, L. X.; Li, K. F.; Wang, H.; Gu, M. J.; Liu, L. S.; Zheng, Z. Z.; Han, N. Y.; Yang, Z. J.; Fan, T. Y. Preparation and in vitro evaluation of a MRI contrast agent based on aptamer-modified gadolinium-loaded liposomes for tumor targeting. *AAPS PharmSciTech* **2017**, *18* (5), 1564−1571.
(34) Yan, H.; Gao, X.; Zhang, Y.; Chang, W.; Li, J.; Li, X.; Du, Q.; Li, C. Imaging tiny hepatic tumor xenografts via endoglin-targeted paramagnetic/optical nanoprobe. *ACS Appl. Mater. Interfaces* **2018**, *10* (20), 17047−17057.
(35) Zu, G.; Cao, Y.; Dong, J.; Zhou, Q.; van Rijn, P.; Liu, M.; Pei, R. Development of an aptamer-conjugated polyrotaxane-based biodegradable magnetic resonance contrast agent for tumor-targeted imaging. *ACS Appl. Bio Mater.* **2019**, *2* (1), 406−416.
(36) Yigit, M. V.; Mazumdar, D.; Kim, H. K.; Lee, J. H.; Odintsov, B.; Lu, Y. Smart "turn-on" magnetic resonance contrast agents based on aptamer-functionalized superparamagnetic iron oxide nanoparticles. *ChemBioChem.* **2007**, *8* (14), 1675−1678.
(37) Yigit, M. V.; Mazumdar, D.; Lu, Y. MRI detection of thrombin with aptamer functionalized superparamagnetic iron oxide nanoparticles. *Bioconjugate Chem.* **2008**, *19* (2), 412−417.
(38) Kim, B.; Yang, J.; Hwang, M.; Choi, J.; Kim, H.-O.; Jang, E.; Lee, J. H.; Ryu, S.-H.; Suh, J.-S.; Huh, Y.-M. Aptamer-modified magnetic nanoprobe for molecular MR imaging of VEGFR2 on angiogenic vasculature. *Nanoscale Res. Lett.* **2013**, *8* (1), 399.
(39) Lim, E. K.; Kim, B.; Choi, Y.; Ro, Y.; Cho, E. J.; Lee, J. H.; Ryu, S. H.; Suh, J. S.; Haam, S.; Huh, Y. M. Aptamer-conjugated magnetic nanoparticles enable efficient targeted detection of integrin $\alpha v\beta 3$ via magnetic resonance imaging. *Journal of Biomedical Materials Research Part A: An Official Journal of The Society for Biomaterials, The Japanese Society for Biomaterials, and The Australian Society for Biomaterials and the Korean Society for Biomaterials* **2014**, *102* (1), 49−59.
(40) Huang, X.; Zhong, J.; Ren, J.; Wen, D.; Zhao, W.; Huan, Y. A DNA aptamer recognizing MMP14 for in vivo and in vitro imaging identified by cell-SELEX. *Oncology Letters* **2019**, *18* (1), 265−274.
(41) Ji, K.; Lim, W. S.; Li, S. F. Y.; Bhakoo, K. A two-step stimulus-response cell-SELEX method to generate a DNA aptamer to recognize inflamed human aortic endothelial cells as a potential in vivo molecular probe for atherosclerosis plaque detection. *Anal. Bioanal. Chem.* **2013**, *405* (21), 6853−6861.
(42) Liu, C. H.; Ren, J.; Liu, C. M.; Liu, P. K. Intracellular gene transcription factor protein-guided MRI by DNA aptamers in vivo. *FASEB J.* **2014**, *28* (1), 464−473.
(43) Zhong, L.; Zou, H.; Huang, Y.; Gong, W.; He, J.; Tan, J.; Lai, Z.; Li, Y.; Zhou, C.; Zhang, G.; et al. Magnetic endoglin aptamer nanoprobe for targeted diagnosis of solid tumor. *J. Biomed. Nanotechnol.* **2019**, *15* (2), 352−362.
(44) Yu, M. K.; Kim, D.; Lee, I. H.; So, J. S.; Jeong, Y. Y.; Jon, S. Image-guided prostate cancer therapy using aptamer-functionalized thermally cross-linked superparamagnetic iron oxide nanoparticles. *Small* **2011**, *7* (15), 2241−2249.
(45) Pilapong, C.; Sitthichai, S.; Thongtem, S.; Thongtem, T. Smart magnetic nanoparticle-aptamer probe for targeted imaging and treatment of hepatocellular carcinoma. *Int. J. Pharm.* **2014**, *473* (1−2), 469−474.
(46) Fang, Y.; Lin, S.; Yang, F.; Situ, J.; Lin, S.; Luo, Y. Aptamer-conjugated multifunctional polymeric nanoparticles as cancer-targeted, MRI-ultrasensitive drug delivery systems for treatment of castration-resistant prostate cancer. *Biomed Res. Int.* **2020**, *2020*, 9186583.
(47) Bernard, E. D.; Beking, M. A.; Rajamanickam, K.; Tsai, E. C.; DeRosa, M. C. Target binding improves relaxivity in aptamer-gadolinium conjugates. *J. Biol. Inorg. Chem.* **2012**, *17* (8), 1159−1175.
(48) Charlton, J.; Sennello, J.; Smith, D. In viva imaging of inflammation using an aptamer inhibitor of human neutrophil elastase. *Chem. Biol.* **1997**, *4* (11), 809−816.
(49) Hicke, B. J.; Stephens, A. W.; Gould, T.; Chang, Y.-F.; Lynott, C. K.; Heil, J.; Borkowski, S.; Hilger, C.-S.; Cook, G.; Warren, S. Tumor targeting by an aptamer. *J. Nucl. Med.* **2006**, *47* (4), 668−678.
(50) Wu, X.; Liang, H.; Tan, Y.; Yuan, C.; Li, S.; Li, X.; Li, G.; Shi, Y.; Zhang, X. Cell-SELEX Aptamer for Highly Specific Radionuclide Molecular Imaging of Glioblastoma In Vivo. *PLoS One* **2014**, *9* (3), No. e90752.
(51) Kryza, D.; Debordeaux, F.; Azéma, L.; Hassan, A.; Paurelle, O.; Schulz, J.; Savona-Baron, C.; Charignon, E.; Bonazza, P.; Taleb, J.; Fernandez, P.; Janier, M.; Toulmé, J. J. Ex Vivo and In Vivo Imaging and Biodistribution of Aptamers Targeting the Human Matrix MetalloProtease-9 in Melanomas. *PLoS One* **2016**, *11* (2), No. e0149387.
(52) Borbas, K. E.; Ferreira, C. S.; Perkins, A.; Bruce, J. I.; Missailidis, S. Design and Synthesis of Mono- and Multimeric Targeted Radiopharmaceuticals Based on Novel Cyclen Ligands Coupled to Anti-MUC1 Aptamers for the Diagnostic Imaging and Targeted Radiotherapy of Cancer. *Bioconjugate Chem.* **2007**, *18* (4), 1205−1212.
(53) Melancon, M. P.; Zhou, M.; Zhang, R.; et al. Selective uptake and imaging of aptamer- and antibody-conjugated hollow nanospheres targeted to epidermal growth factor receptors overexpressed in head and neck cancer. *ACS Nano* **2014**, *8* (5), 4530−4538.
(54) Garcia, E. V. Physical attributes, limitations, and future potential for PET and SPECT. *Journal of Nuclear Cardiology* **2012**, *19*, 19−29.
(55) Rong, J.; Haider, A.; Jeppesen, T. E.; Josephson, L.; Liang, S. H. Radiochemistry for positron emission tomography. *Nat. Commun.* **2023**, *14* (1), 3257.
(56) Shukla, A. K.; Kumar, U. Positron emission tomography: An overview. *Journal of Medical Physics* **2006**, *31* (1), 13−21.
(57) Ter-Pogossian, M. M.; Phelps, M. E.; Hoffman, E. J.; et al. A positron-emission transaxial tomograph for nuclear imaging (PETT). *Radiology* **1975**, *114* (1), 89−98.
(58) Phelps, M. E.; Hoffman, E. J.; Mullani, N. A.; Ter-Pogossian, M. M. Application of annihilation coincidence detection to transaxial reconstruction tomography. *J. Nucl. Med.* **1975**, *16* (3), 210−224.
(59) Rockey, W. M.; Huang, L.; Kloepping, K. C.; Baumhover, N. J.; Giangrande, P. H.; Schultz, M. K. Synthesis and radiolabeling of chelator-RNA aptamer bioconjugates with copper-64 for targeted molecular imaging. *Bioorg. Med. Chem.* **2011**, *19* (13), 4080−4090.
(60) Li, J.; Zheng, H.; Bates, P. J.; Malik, T.; Li, X. F.; Trent, J. O.; Ng, C. K. Aptamer imaging with Cu-64 labeled AS1411: Preliminary assessment in lung cancer. *Nucl. Med. Biol.* **2014**, *41* (2), 179−185.
(61) Jacobson, O.; Yan, X.; Niu, G.; Weiss, I. D.; Ma, Y.; Szajek, L. P.; Shen, B.; Kiesewetter, D. O.; Chen, X. PET Imaging of Tenascin-C with a Radiolabeled Single-Stranded DNA Aptamer. *J. Nucl. Med.* **2015**, *56* (4), 616−621.
(62) Kim, H. J.; Park, J. Y.; Lee, T. S.; Song, I. H.; Cho, Y. L.; Chae, J. R.; Kang, H.; Lim, J. H.; Lee, J. H.; Kang, W. J. PET imaging of HER2 expression with an 18F-fluoride labeled aptamer. *PLoS One* **2019**, *14* (1), No. e0211047.
(63) Gijs, M.; Becker, G.; Plenevaux, A. Biodistribution of Novel ^{68}Ga-Radiolabelled HER2 Aptamers in Mice. *Journal of Nuclear Medicine & Radiation Therapy* **2016**, *7* (5), 1000300.
(64) Ding, D.; Zhao, H.; Wei, D.; Yang, Q.; Yang, C.; Wang, R.; Chen, Y.; Li, L.; An, S.; Xia, Q.; et al. The first-in-human whole-body dynamic pharmacokinetics study of Aptamer. *Research* **2023**, *6*, 0126.
(65) Foudas, A. W.; Kosheleva, R. I.; Favvas, E. P.; Kostoglou, M.; Mitropoulos, A. C.; Kyzas, G. Z. Fundamentals and applications of nanobubbles: A review. *Chem. Eng. Res. Des.* **2023**, *189*, 64−86.
(66) Kyzas, G. Z.; Mitropoulos, A. C. From Bubbles to Nanobubbles. *Nanomaterials* **2021**, *11* (10), 2592.
(67) Goodwin, A. P.; Nakatsuka, M. A.; Mattrey, R. F. Stimulus-responsive ultrasound contrast agents for clinical imaging: motivations, demonstrations, and future directions. *WIREs Nanomed. Nanobiotechnol.* **2015**, *7* (1), 111−123.

(68) Wang, C.-H.; Huang, Y.-F.; Yeh, C.-K. Aptamer-Conjugated Nanobubbles for Targeted Ultrasound Molecular Imaging. *Langmuir* **2011**, *27* (11), 6971−6976.
(69) Wang, C.-H.; Kang, S.-T.; Lee, Y.-H.; Luo, Y.-L.; Huang, Y.-F.; Yeh, C.-K. Aptamer-conjugated and drug-loaded acoustic droplets for ultrasound theranosis. *Biomaterials* **2012**, *33* (6), 1939−1947.
(70) Nakatsuka, M. A.; Mattrey, R. F.; Esener, S. C.; Cha, J. N.; Goodwin, A. P. Aptamer-Crosslinked Microbubbles: Smart Contrast Agents for Thrombin-Activated Ultrasound Imaging. *Adv. Mater.* **2012**, *24* (45), 6010−6016.
(71) Nakatsuka, M. A.; Barback, C. V.; Fitch, K. R.; Farwell, A. R.; Esener, S. C.; Mattrey, R. F.; Cha, J. N.; Goodwin, A. P. In vivo ultrasound visualization of non-occlusive blood clots with thrombin-sensitive contrast agents. *Biomaterials* **2013**, *34* (37), 9559−9565.
(72) Wu, M.; Wang, Y.; Wang, Y.; Zhang, M.; Luo, Y.; Tang, J.; Wang, Z.; Wang, D.; Hao, L.; Wang, Z. Paclitaxel-loaded and A10−3.2 aptamer-targeted poly(lactide-co-glycolic acid) nanobubbles for ultrasound imaging and therapy of prostate cancer. *Int. J. Nanomed.* **2017**, *12*, 5313−5330.
(73) Pasternak, J. J.; Williamson, E. E. In *Clinical pharmacology, uses, and adverse reactions of iodinated contrast agents: a primer for the non-radiologist*; Mayo Clinic Proceedings; Elsevier, 2012; pp 390−402.
(74) Curry, T.; Kopelman, R.; Shilo, M.; Popovtzer, R. Multifunctional theranostic gold nanoparticles for targeted CT imaging and photothermal therapy. *Contrast Media Mol. Imaging* **2014**, *9* (1), 53−61.
(75) Kim, D.; Jeong, Y. Y.; Jon, S. A drug-loaded aptamer-gold nanoparticle bioconjugate for combined CT imaging and therapy of prostate cancer. *ACS Nano* **2010**, *4* (7), 3689−3696.
(76) Li, C. H.; Kuo, T.-R.; Su, H. J.; Lai, W. Y.; Yang, P. C.; Chen, J. S.; Wang, D. Y.; Wu, Y. C.; Chen, C. C. Fluorescence-Guided Probes of Aptamer-Targeted Gold Nanoparticles with Computed Tomography Imaging Accesses for in Vivo Tumor Resection. *Sci. Rep.* **2015**, *5* (1), 15675.
(77) Mohammadzadeh, P.; Cohan, R. A.; Ghoreishi, S. M.; Bitarafan-Rajabi, A.; Ardestani, M. S. AS1411 Aptamer-Anionic Linear Globular Dendrimer G2-Iohexol Selective Nano-Theranostics. *Sci. Rep.* **2017**, *7* (1), 11832.
(78) Alibolandi, M.; Hoseini, F.; Mohammadi, M.; Ramezani, P.; Einafshar, E.; Taghdisi, S. M.; Ramezani, M.; Abnous, K. Curcumin-entrapped MUC-1 aptamer targeted dendrimer-gold hybrid nanostructure as a theranostic system for colon adenocarcinoma. *Int. J. Pharm.* **2018**, *549* (1−2), 67−75.
(79) Cao, Y.; Wu, T.; Dai, W.; Dong, H.; Zhang, X. TiO2 Nanosheets with the Au Nanocrystal-Decorated Edge for Mitochondria-Targeting Enhanced Sonodynamic Therapy. *Chem. Mater.* **2019**, *31* (21), 9105−9114.
(80) Hirao, I.; Kimoto, M.; Mitsui, T.; Fujiwara, T.; Kawai, R.; Sato, A.; Harada, Y.; Yokoyama, S. An unnatural hydrophobic base pair system: site-specific incorporation of nucleotide analogs into DNA and RNA. *Nat. Methods* **2006**, *3* (9), 729−735.
(81) Malyshev, D. A.; Dhami, K.; Lavergne, T.; Chen, T.; Dai, N.; Foster, J. M.; Corrêa, I. R.; Romesberg, F. E. A semi-synthetic organism with an expanded genetic alphabet. *Nature* **2014**, *509* (7500), 385−388.
(82) Yang, Z.; Sismour, A. M.; Sheng, P.; Puskar, N. L.; Benner, S. A. Enzymatic incorporation of a third nucleobase pair. *Nucleic Acids Res.* **2007**, *35* (13), 4238−4249.
(83) Sefah, K.; Yang, Z.; Bradley, K. M.; Hoshika, S.; Jiménez, E.; Zhang, L.; Zhu, G.; Shanker, S.; Yu, F.; Turek, D.; et al. In vitro selection with artificial expanded genetic information systems. *Proc. Natl. Acad. Sci. U. S. A.* **2014**, *111* (4), 1449−1454.
(84) Zhang, L.; Yang, Z.; Sefah, K.; Bradley, K. M.; Hoshika, S.; Kim, M. J.; Kim, H. J.; Zhu, G.; Jiménez, E.; Cansiz, S.; et al. Evolution of functional six-nucleotide DNA. *J. Am. Chem. Soc.* **2015**, *137* (21), 6734−6737.
(85) Ren, X.; Gelinas, A. D.; von Carlowitz, I.; Janjic, N.; Pyle, A. M. Structural basis for IL-1α recognition by a modified DNA aptamer that specifically inhibits IL-1α signaling. *Nat. Commun.* **2017**, *8* (1), 810.

https://doi.org/10.1021/cbmi.4c00103
Chem. Biomed. Imaging 2025, 3, 267−279